Nucleon-nucleon scattering parameters in the limit of SU(3) flavor symmetry

Nucleon-nucleon scattering parameters in the limit of SU(3) flavor symmetry

S. R. Beane,[1] E. Chang,[2] S. D. Cohen,[2] W. Detmold,[3] P. Junnarkar,[4] H. W. Lin,[2] T. C. Luu,[5] K. Orginos,[6,7] A. Parreño,[8] M. J. Savage,[1,2] and A. Walker-Loud[9,10]
(NPLQCD Collaboration)

[1]*Helmholtz-Institut für Strahlen- und Kernphysik (Theorie), Universität Bonn, D-53115 Bonn, Germany*
[2]*Department of Physics, University of Washington, Box 351560, Seattle, Washington 98195, USA*
[3]*Center for Theoretical Physics, Massachusetts Institute of Technology, Cambridge, Massachusetts 02139, USA*
[4]*Department of Physics, University of New Hampshire, Durham, New Hampshire 03824-3568, USA*
[5]*N Section, Lawrence Livermore National Laboratory, Livermore, California 94551, USA*
[6]*Department of Physics, College of William and Mary, Williamsburg, Virginia 23187-8795, USA*
[7]*Jefferson Laboratory, 12000 Jefferson Avenue, Newport News, Virginia 23606, USA*
[8]*Departamento d'Estructura i Constituents de la Matèria, Institut de Ciències del Cosmos (ICC), Universitat de Barcelona, Martí i Franquès 1, E08028 Barcelona, Spain*
[9]*Lawrence Berkeley National Laboratory, Berkeley, California 94720, USA*
[10]*Department of Physics, University of California, Berkeley, California 94720, USA*

(Received 21 February 2013; revised manuscript received 19 June 2013; published 21 August 2013)

The scattering lengths and effective ranges that describe low-energy nucleon-nucleon scattering are calculated in the limit of SU(3)-flavor symmetry at the physical strange-quark mass with lattice quantum chromodynamics. The calculations are performed with an isotropic clover discretization of the quark action in three volumes with spatial extents of $L \sim 3.4$ fm, 4.5 fm, and 6.7 fm, and with a lattice spacing of $b \sim 0.145$ fm. With determinations of the energies of the two-nucleon systems (both of which contain bound states at these up and down quark masses) at rest and moving in the lattice volume, Lüscher's method is used to determine the low-energy phase shifts in each channel, from which the scattering length and effective range are obtained. The scattering parameters, in the ${}^1S_0$ channel are found to be $m_\pi a^{({}^1S_0)} = 9.50^{+0.78+1.10}_{-0.69-0.80}$ and $m_\pi r^{({}^1S_0)} = 4.61^{+0.29+0.24}_{-0.31-0.26}$, and in the ${}^3S_1$ channel are $m_\pi a^{({}^3S_1)} = 7.45^{+0.57+0.71}_{-0.53-0.49}$ and $m_\pi r^{({}^3S_1)} = 3.71^{+0.28+0.28}_{-0.31-0.35}$. These values are consistent with the two-nucleon system exhibiting Wigner's supermultiplet symmetry, which becomes exact in the limit of large N_c. In both spin channels, the phase shifts change sign at higher momentum, near the start of the t-channel cut, indicating that the nuclear interactions have a repulsive core even at the SU(3)-symmetric point.

DOI: 10.1103/PhysRevC.88.024003 PACS number(s): 12.38.Gc, 13.75.Cs, 13.85.−t, 25.10.+s

I. INTRODUCTION

Decades of experimental measurements of the nucleon-nucleon (NN) cross sections have resulted in precise phase shifts and scattering parameters that provide the cornerstone of nuclear physics. These two-body interactions, when combined with multibody interactions, dictate the low-energy spectra and interactions of nuclei, and also the equation of state of nuclear matter at moderate densities. Further, these interactions are responsible for the fine-tunings that permeate nuclear physics, and are responsible for producing sufficient carbon in the universe to allow for the emergence of life. During the last several years, there has been a substantial effort to determine the *NN* interactions directly from quantum chromodynamics (QCD) using the numerical technique of lattice QCD (LQCD) [1–14]. Steady progress is being made toward this objective, but calculations at the physical light-quark masses have not yet been performed, and essentially only one lattice spacing has been used in calculations. While calculations at the physical light-quark masses—that are extrapolated to the continuum limits and are performed in volumes (and temporal directions) that are much larger than the inverse Compton wavelength of the pion—are required to verify the LQCD technology and provide a rigorous underpinning of modern nuclear interactions, calculations at heavier pion masses are equally important in understanding and quantifying the fine-tunings in nuclear physics. It is crucial to understand how the fine-tunings in nuclear physics translate into constraints on the five relevant fundamental parameters in the standard model of particle physics: the three light-quark masses, and the strong and electromagnetic coupling constants. The *NN* interaction provides the simplest place to begin this investigation.

One reason that there are presently few LQCD calculations of *NN* interactions is the significantly greater complexity of multinucleon systems as compared with systems of single mesons and baryons. A second reason is that significant computational resources are required to generate high-quality ensembles of gauge field configurations at or near the physical light-quark masses, an effort that has only become practical with the availability of petascale computers, and, as yet, these ensembles are not at sufficiently large volume to be of use in nuclear physics. At heavier quark masses, the resources required to generate ensembles of lattice gauge configurations and light-quark propagators are relatively small, the degradation of the signal-to-noise in multinucleon correlation functions is significantly reduced, and thermal effects are exponentially suppressed, compared to calculations at lighter pion masses. For these reasons, we performed LQCD calculations of a number of s-shell nuclei and hypernuclei with $A \leqslant 5$ at the SU(3)-flavor symmetry point with the physical

TABLE I. Parameters of the ensembles of gauge-field configurations and of the measurements used in this work. The lattices have dimension $L^3 \times T$, a lattice spacing b, and a bare quark mass $b\,m_q$ (in lattice units) generating a pion of mass m_π. $N_{\rm src}$ light-quark sources are used (as described in the text) to perform measurements on $N_{\rm cfg}$ configurations in each ensemble. The three uncertainties associated with the pion mass are statistical, fitting systematic, and that associated with the lattice spacing, respectively.

Label	L/b	T/b	β	$b\,m_q$	b (fm)	L (fm)	T (fm)	m_π (MeV)	$m_\pi L$	$m_\pi T$	$N_{\rm cfg}$	$N_{\rm src}$
A	24	48	6.1	−0.2450	0.145	3.4	6.7	806.5(0.3)(0)(8.9)	14.3	28.5	3822	96
B	32	48	6.1	−0.2450	0.145	4.5	6.7	806.9(0.3)(0.5)(8.9)	19.0	28.5	3050	72
C	48	64	6.1	−0.2450	0.145	6.7	9.0	806.7(0.3)(0)(8.9)	28.5	38.0	1905	54

strange quark mass giving $m_\pi = 805.9(0.6)(0.4)(8.9)$ MeV, at a lattice spacing of $b \sim 0.145$ fm, and in lattice volumes with spatial extents $L \sim 3.4$ fm, 4.5 fm and 6.7 fm [13]. In this work, we continue this study and explore the NN scattering phase shifts below the inelastic threshold and the associated scattering parameters relevant below the t-channel cut at the SU(3) symmetric point.

II. OVERVIEW OF THE LATTICE QCD CALCULATIONS

Three ensembles of isotropic gauge-field configurations, generated with a tadpole-improved Lüscher-Weisz gauge action and a clover fermion action [15], are used in this work and have been used previously to calculate the lowest-lying levels of the s-shell nuclei and hypernuclei [13]. This particular lattice-action setup follows closely the anisotropic clover action of the ensembles generated by the JLab group that we have used in our previous calculations [4,11,16–19]. The parameter tuning and scaling properties of this action will be discussed elsewhere [20]. One level of stout smearing [21] with $\rho = 0.125$ and tadpole-improved tree-level clover coefficient $c_{\rm SW} = 1.2493$ are used in the gauge-field generation. Studies [20,22,23] of the partially conserved axial-current (PCAC) relation in the Schrödinger functional indicate that this choice is consistent with vanishing $\mathcal{O}(b)$ violations, leading to discretization effects that are essentially $\mathcal{O}(b^2)$. The parameters of the ensembles are listed in Table I, and further details will be presented elsewhere [20]. As two-nucleon systems are the focus of this work, relatively large lattice volumes are employed for the calculations, with correspondingly large values of $m_\pi L$ and $m_\pi T$. In order to convert the calculated energies from lattice units (l.u.) into physical units (MeV), a lattice spacing of $b = 0.1453(16)$ fm has been determined for these ensembles of gauge-field configurations from the Υ spectrum [24].

The $N_{\rm cfg}$ gauge configurations in each of the ensembles are separated by ten hybrid Monte Carlo (HMC) evolution trajectories to reduce autocorrelations, and an average of $N_{\rm src}$ measurements are performed on each configuration. The quark propagators are constructed with gauge-invariant Gaussian-smeared sources with stout-smeared gauge links. These sources are distributed over a grid, the center of which is randomly distributed within the lattice volume on each configuration, and the quark propagators are computed using the BiCGstab algorithm with a tolerance of 10^{-12} in double precision. Quark propagators, either unsmeared or smeared at the sink using the same parameters as used at the source, give rise to two sets of correlation functions for each combination of source and sink interpolating fields, labeled as SP and SS, respectively. The propagators are contracted to form nucleon blocks projected to fixed momentum at the sink for use in the calculation of the correlation functions. The blocks are defined as

$$\mathcal{B}_N^{ijk}(\mathbf{p}, t; x_0) = \sum_{\mathbf{x}} e^{i\mathbf{p}\cdot\mathbf{x}} S_i^{(f_1),i'}(\mathbf{x}, t; x_0) S_j^{(f_2),j'}(\mathbf{x}, t; x_0) S_k^{(f_3),k'} \times (\mathbf{x}, t; x_0) b^{(N)}_{i'j'k'}, \quad (1)$$

where $S^{(f)}$ is a quark propagator of flavor f, and the indices are combined spin-color indices running over $i = 1, \ldots, N_c N_s$.[1] The choice of the f_i and the tensor $b^{(N)}$ depend on the spin and isospin of the nucleon under consideration. For our

[1] To be specific, for a quark spin component $i_s = 1, \ldots, N_s$ and color component $i_c = 1, \ldots, N_c$, the combined index $i = N_c(i_s - 1) + i_c$.

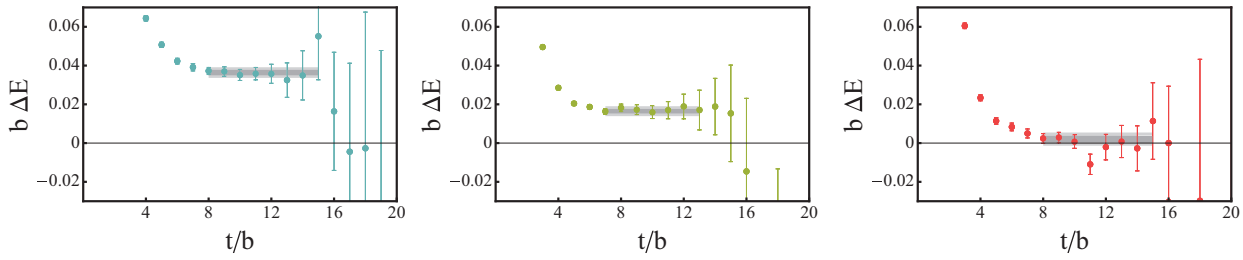

FIG. 1. (Color online) The EMPs of the first excited states with $|\mathrm{P}| = 0$ in the $^1S_0$ channel in the $L = 3.4$ fm, $L = 4.5$ fm, and $L = 6.7$ fm ensembles, respectively. Twice the nucleon mass has been subtracted from the energy. The dark (light) shaded regions correspond to the statistical uncertainty (statistical and systematic uncertainties combined in quadrature) of the fit to the plateau over the indicated time interval.

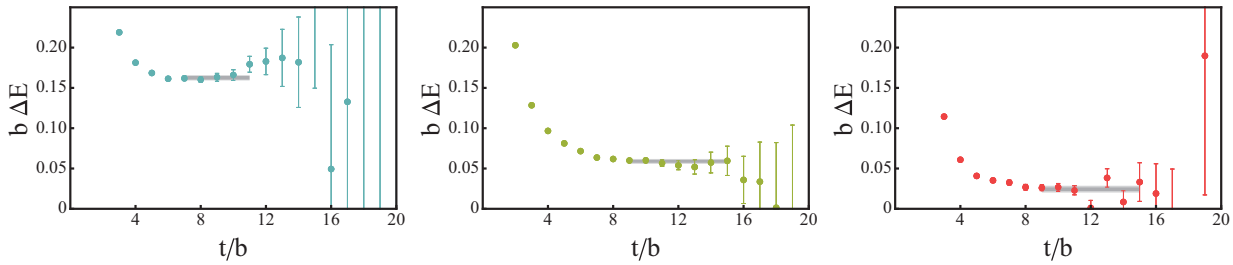

FIG. 2. (Color online) The EMPs of the first excited state with $|\mathrm{P}| = 1$ in the $^1S_0$ channel in the $L = 3.4$ fm, $L = 4.5$ fm, and $L = 6.7$ fm ensembles, respectively. Twice the nucleon mass has been subtracted from the energy. The dark (light) shaded regions correspond to the statistical uncertainty (statistical and systematic uncertainties combined in quadrature) of the fit to the plateau over the indicated time interval.

calculations we used the local interpolating fields constructed in Ref. [25], restricted to those that contain only upper spin components (in the Dirac spinor basis). This choice results in the simplest interpolating fields that also have the best overlap with the nucleon ground states. Blocks are constructed for all lattice momenta $|\mathbf{p}|^2 < 4$ allowing for the study of multinucleon systems with zero or nonzero total momentum and with nontrivial spatial wave functions. Interpolating operators used at the sink have blocks with back-to-back momentum to access excited states. These interpolating operators have small overlaps onto the ground state, and it is found that the correlation functions from these back-to-back interpolating operators are as well fit by single states as are the ground-state correlation functions. More sophisticated methods such as Matrix Prony [26] and GPoF [27,28] have been applied to the correlation functions and do not provide significant improvement in the extractions, indicating that the correlators with back-to-back momenta are close to orthogonal. Future investigations with a fully variational basis of operators are required to give us confidence in extracting states beyond the first excitation. The dispersion relations of the single mesons and nucleons on these ensembles have been examined in Ref. [13], and the infinite volume extrapolations of the masses are $m_\pi = 0.59426(12)(11)$ l.u. $=$ 805.9(0.6)(0.4)(8.9) MeV and $M_N = 1.20359(41)(61)$ l.u. $=$ 1.635(0)(0)(18) GeV.

III. NUCLEON-NUCLEON SCATTERING IN THE $^1S_0$ CHANNEL

In contrast to the real world, there is a bound state in the $^1S_0$ channel at the SU(3)-symmetric point with a binding energy of $B_{nn} = 15.9(2.7)(2.7)(0.2)$ MeV [13].[2] Two-nucleon correlation functions with total momentum[3] $|\mathrm{P}| = 0$ and $|\mathrm{P}| = 1$ evaluated in three lattice volumes, with spatial extent $L = 3.4$ fm, 4.5 fm, and 6.7 fm, are used to extract the binding energy of the dineutron. While the results are found to be consistent, volume effects are observed in the smallest volume, and the binding energy determined in the largest volume is taken as the infinite volume value. In the largest volume, the exponentially suppressed deviations from the infinite volume value are negligible for this binding energy. With one bound state in this channel, Levinson's theorem dictates that the phase shift is $\delta^{(^1S_0)}(0) = \pi$ at threshold.

While the location of the bound state does not correspond to a real value for the scattering phase shift, it does provide a real value of $k \cot \delta$, and a valuable constraint on the scattering parameters in the effective range expansion, which is valid below the t-channel cut starting at $|\mathbf{k}| = m_\pi/2$. Positively shifted energy eigenvalues of two-body systems in the lattice volumes can be related to scattering phase shifts using Lüscher's relation [31–33] and its extension to boosted systems [34–37] provided they lie below the inelastic threshold. The effective mass plots (EMPs) associated with

[2]It should be noted that the HALQCD Collaboration does not find a bound state in the $^1S_0$ channel nor $^3S_1$-$^3D_1$ coupled-channels at this pion mass [12]. Their results are arrived at through the solution of the Schrödinger equation with "potentials" calculated on the lattice, a method which is theoretically unsound in various ways [29,30], and, moreover, is considerably less direct than determining binding energies using simple spectroscopy.

[3]Here, $|\mathrm{P}|$ denotes the magnitude of the total momentum in units of $2\pi/L$.

TABLE II. Results from the lowest-lying continuum states in the $^1S_0$ channel.

Ensemble	$\lvert\mathrm{P}\rvert$	$b\Delta E$	$\lvert\mathbf{k}\rvert/m_\pi$	$k \cot \delta/m_\pi$	δ (deg)
$24^3 \times 48$	0	0.0358(13)(16)	0.3506(64)(78)	$0.175^{+.034\ +0.043}_{-0.031-0.036}$	63.4(3.8)(4.7)
$24^3 \times 48$	1	0.1609(16)(37)	0.7197(41)(93)	$-0.30^{+0.07+0.15}_{-0.07-0.17}$	$-67(5)(11)$
$32^3 \times 48$	0	0.0165(13)(22)	0.2373(92)(96)	$0.030^{+0.031+0.057}_{-0.028-0.046}$	83(7)(13)
$32^3 \times 48$	1	0.0591(23)(46)	0.420(09)(19)		
$48^3 \times 64$	0	0.0020(18)(29)			
$48^3 \times 64$	1	0.0244(24)(35)	0.267(15)(23)		

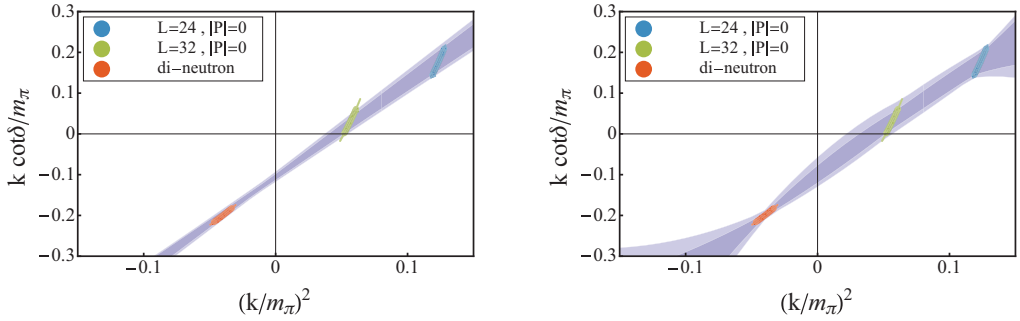

FIG. 3. (Color online) $k \cot \delta$ in the $^1S_0$ channel. The positive energy values are given in Table II and the negative energy value is determined from the dineutron binding energy. The left panel is a two-parameter fit to the ERE, and the right panel is a three-parameter fit to the ERE, as described in the text. The inner (outer) shaded region corresponds to the statistical uncertainty (statistical and systematic uncertainties combined in quadrature).

the two-nucleon energy, reduced by twice the nucleon mass, of the first excited states with $|\mathrm{P}| = 0$ are shown in Fig. 1. Plateaus in the EMPs are found in all volumes, leading to clean extractions of the energy splitting, and also to values of the phase shift via Lüscher's eigenvalue equation at those energies in the $L = 3.4$ fm and $L = 4.5$ fm ensembles. The energy splitting in the $L = 6.7$ fm ensemble is consistent with zero, and therefore straddles the lowest singularity in the eigenvalue equation, thereby providing no meaningful constraint on the phase shift or $k \cot \delta$. The energy splittings are determined with a correlated χ^2-minimization fit of a constant to the plateau in the EMPs over the fit ranges shown in Fig. 1. Jackknife resampling is used to generate the covariance matrix required to define χ^2 from the correlation functions. Consistent results for the extracted values of the energies are obtained using both one- and two-state exponential fits to the correlation functions. In the figures, the inner shaded region corresponds to the statistical uncertainty in the fit, derived from the χ^2 minimization, and the outer uncertainty corresponds to the fitting systematic uncertainty combined in quadrature with the statistical uncertainty. The fitting systematic uncertainty is determined by varying the fitting interval over the extent of the plateau region and accommodating the range of central fit values. The EMPs associated with the first excited state with $|\mathrm{P}| = 1$ are shown in Fig. 2. The correlation functions in the $L = 4.5$ fm and 6.7 fm ensembles are not sufficiently precise to provide a statistically meaningful phase shift, as the energies are near singularities in Lüscher's eigenvalue equation. This demonstrates a significant difficulty in determining phase shifts in large volumes where the poles of the eigenvalue equation are collapsing to form the infinite-volume scattering continuum. Table II shows the results extracted from the lowest-lying continuum levels from each of the ensembles.

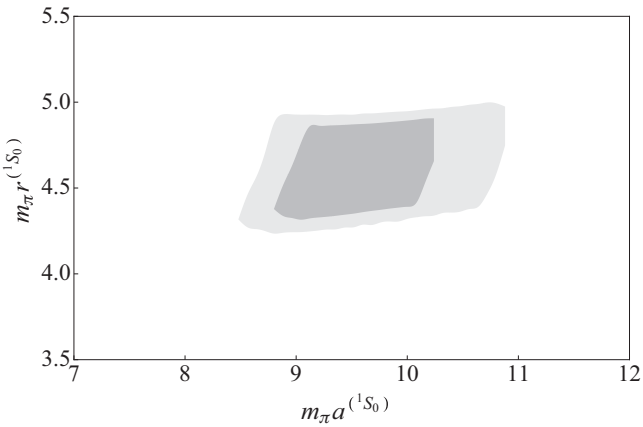

FIG. 4. The 68% confidence region associated with $m_\pi a^{(^1S_0)}$ and $m_\pi r^{(^1S_0)}$ in the $^1S_0$ channel. The inner region corresponds to statistical uncertainties and the outer region corresponds to statistical and systematic uncertainties combined in quadrature.

Below the inelastic threshold, at $|\mathbf{k}|^2 = M_N m_\pi + m_\pi^2/4$, where k is the magnitude of the three-momentum of each nucleon in the center-of-mass (CoM) frame, the s-wave scattering amplitude can be uniquely described by a single phase shift and more directly $k \cot \delta$. Near threshold, and more generally, below the t-channel cut, $k \cot \delta$ has a power-series expansion in terms of the kinetic energy of the two-nucleons,

$$k \cot \delta = -\frac{1}{a} + \frac{1}{2} r |\mathbf{k}|^2 + P |\mathbf{k}|^4 + \mathcal{O}(|\mathbf{k}|^6), \qquad (2)$$

called the effective range expansion (ERE), where a is the scattering length (using the nuclear physics sign convention), r is the effective range and P is the shape parameter. While the range of possible values of the scattering length is unbounded, the size of the effective range and shape parameter are set by the range of the interaction. In Fig. 3, the extracted values of $k \cot \delta / m_\pi$ given in Table II for $|\mathrm{P}| = 0$ and from the dineutron binding energy are shown as a function of $|\mathbf{k}|^2/m_\pi^2$. The three points shown in Fig. 3 lie significantly below the t-channel cut and so the ERE of $k \cot \delta$ can be fit to define the phase shift throughout this kinematic regime. With three points to fit, two-parameter (left panel) and three-parameter (right panel) fits to the ERE of $k \cot \delta / m_\pi$ are performed and are shown as the shaded regions in Fig. 3.

The successful description by a two-parameter fit indicates small values of the terms that are higher order in the ERE, consistent with what is observed at the physical pion mass. The scattering length and effective range determined from the two-parameter fit are

$$m_\pi a^{(^1S_0)} = 9.50^{+0.78+1.10}_{-0.69-0.80}, \quad m_\pi r^{(^1S_0)} = 4.61^{+0.29+0.24}_{-0.31-0.26}, \qquad (3)$$

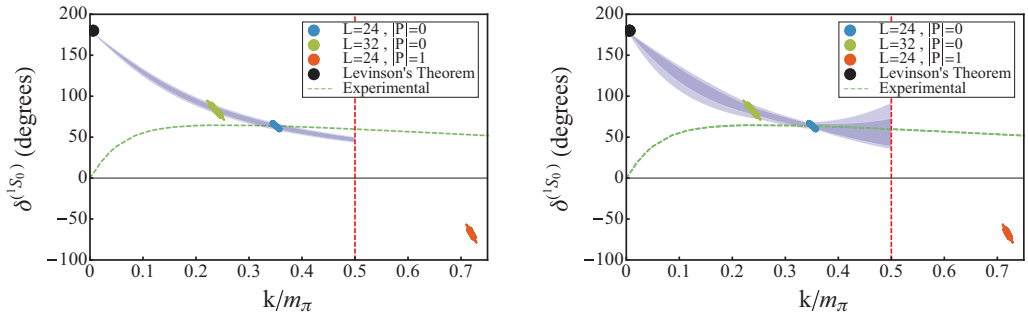

FIG. 5. (Color online) The phase shift in the $^1S_0$ channel. The left panel is a two-parameter fit to the ERE, while the right panel is a three-parameter fit to the ERE, as described in the text. The inner (outer) shaded region corresponds to the statistical uncertainty (statistical and systematic uncertainties combined in quadrature) in two- and three-parameter ERE fits to the results of the lattice QCD calculation. The vertical (red) dashed line corresponds to the start of the t-channel cut and the upper limit of the range of validity of the ERE. The light (green) dashed line corresponds to the phase shift at the physical pion mass from the Nijmegen phase-shift analysis [38].

corresponding to

$$a^{(^1S_0)} = 2.33^{+0.19+0.27}_{-0.17-0.20}\ \text{fm}, \quad r^{(^1S_0)} = 1.130^{+0.071+0.059}_{-0.077-0.063}\ \text{fm}. \quad (4)$$

The uncertainties associated with $a^{(^1S_0)}$ and $r^{(^1S_0)}$ are correlated, and their 68% confidence region is shown in Fig. 4. The uncertainty in the scattering length is asymmetric as it is the inverse scattering length that is the fit parameter. The shape parameter obtained from the three parameter fit to the ERE expansion is consistent with zero: $Pm_\pi^3 = -1^{+4+5}_{-5-8}$. The scattering length and effective range extracted from the three-parameter fit are consistent with the two-parameter fit, but with larger uncertainties. A full quantification of the theoretical error in the determination of the ERE parameters requires more calculations than are currently available.

The phase shift below the t-channel cut can be determined from these fit parameters, and is shown in Fig. 5, along with the results of the LQCD calculations and the phase shift at the physical values of the quark masses. We expect the phase shift predicted by the ERE to deviate significantly from the true phase shift near the start of the t-channel cut, and this is indeed suggested by Fig. 5. Like the phase shift at the physical point, the phase shift at the SU(3) symmetric point is found to change sign at larger momenta, consistent with the presence of a repulsive hard core in the NN interaction.

IV. NUCLEON-NUCLEON SCATTERING IN THE $^3S_1$-$^3D_1$ COUPLED CHANNELS

At the SU(3)-symmetric point, the deuteron is bound [13] by $B = 19.5(3.6)(3.1)(0.2)$ MeV which, as with the bound dineutron in the $^1S_0$ channel, provides a constraint on $k \cot \delta$. The deuteron has a d-wave component induced by the tensor interaction, however mixing between the s wave and the d wave is higher order in the ERE and first appears at the same order as the shape parameter [39]. Therefore, while the scattering length and effective range are purely s wave, the shape parameter is contaminated by the d-wave admixture. The EMPs associated with the first excited states with $|\mathrm{P}| = 0$ are shown in Fig. 6, and with $|\mathrm{P}| = 1$ are shown in Fig. 7. The correlation functions calculated on the $L = 6.7$ fm ensemble have energies that are too close to, or straddle, the singularities of Lüscher's eigenvalue equation and are not useful in determining the phase shift. The results extracted from the fits to the plateau regions in these EMPs are given in Table III.

In Fig. 8, the extracted values of $k \cot \delta / m_\pi$ given in Table III and from the deuteron binding energy are shown as a function of $|\mathbf{k}|^2/m_\pi^2$. Following the procedure used to analyze the results in the $^1S_0$ channel, again with three points to fit, two-parameter (left panel) and three-parameter (right panel) fits to the ERE of $k \cot \delta / m_\pi$ are performed and shown as the shaded regions in Fig. 8. The scattering length and effective

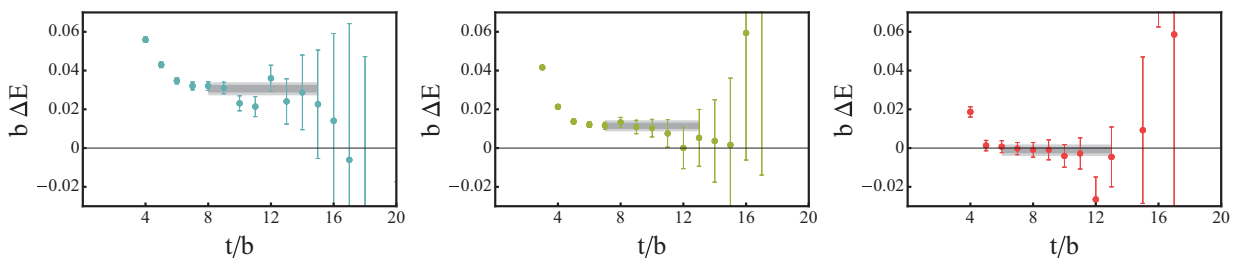

FIG. 6. (Color online) The EMPs of the first excited states with $|\mathrm{P}| = 0$ in the $^3S_1$ channel in the $L = 3.4$ fm, $L = 4.5$ fm, and $L = 6.7$ fm ensembles, respectively. Twice the nucleon mass has been subtracted from the energy. The dark (light) shaded regions correspond to the statistical uncertainty (statistical and systematic uncertainties combined in quadrature) of the fit to the plateau over the indicated time interval.

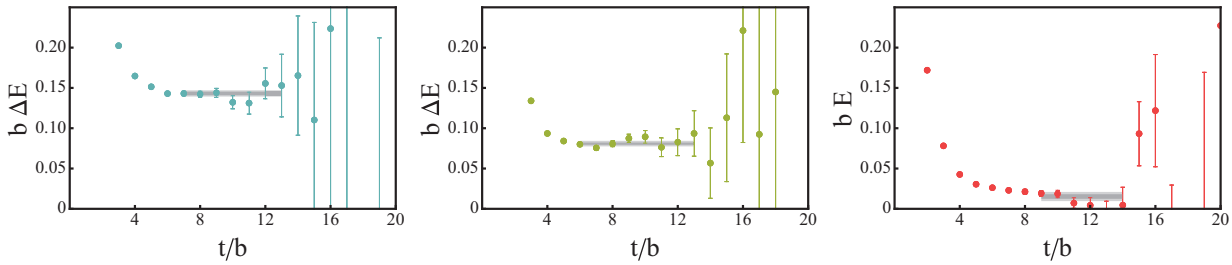

FIG. 7. (Color online) The EMPs of the first excited states with $|\mathrm{P}| = 1$ in the $^3S_1$ channel in the $L = 3.4$ fm, $L = 4.5$ fm, and $L = 6.7$ fm ensembles, respectively. Twice the nucleon mass has been subtracted from the energy. The dark (light) shaded regions correspond to the statistical uncertainty (statistical and systematic uncertainties combined in quadrature) of the fit to the plateau over the indicated time interval.

range determined from the two-parameter fit are

$$m_\pi a^{(^3S_1)} = 7.45^{+0.57+0.71}_{-0.53-0.49}\,, \quad m_\pi r^{(^3S_1)} = 3.71^{+0.28+0.28}_{-0.31-0.35}\,, \tag{5}$$

corresponding to

$$\begin{aligned} a^{(^3S_1)} &= 1.82^{+0.14+0.17}_{-0.13-0.12}\ \text{fm}, \\ r^{(^3S_1)} &= 0.906^{+0.068+0.068}_{-0.075-0.084}\ \text{fm}, \end{aligned} \tag{6}$$

and Fig. 9 shows the 68% confidence region for the extracted values of $a^{(^3S_1)}$ and $r^{(^3S_1)}$. The shape parameter obtained from the three parameter fit to the ERE expansion is consistent with zero: $Pm_\pi^3 = 2^{+5+5}_{-6-6}$. Again the scattering length and effective range extracted from the three-parameter fit are consistent with the two-parameter fit, but with larger uncertainties.

The phase shift below the t-channel cut can be determined from these fit parameters, and is shown in Fig. 10, along with the results of the LQCD calculations and the phase shift at the physical point. As in the $^1S_0$ channel, the phase shift predicted by the ERE is expected to deviate significantly from the true phase shift near the t-channel cut, and this is seen in Fig. 10. Like the $^3S_1$ phase shift at the physical point, and the phase shift we have obtained in the $^1S_0$ channel, the phase shift at the SU(3) symmetric point is found to change sign at larger momenta, consistent with the presence of a repulsive hard core in the NN interaction.

V. NUCLEON-NUCLEON EFFECTIVE RANGES

Unlike the scattering length, the size of the effective range and the higher-order contributions to the ERE are set by the range of the interaction. The leading estimate of the effective range for light quarks is $r \sim 1/m_\pi$, and higher-order contributions are expected to be suppressed by further powers of the light-quark masses. It is natural to consider an expansion of the product $m_\pi r$ in the light-quark masses. While the most general form of the expansion contains terms that are nonanalytic in the pion mass [40–43], for instance of the form $m_q \log m_q$, with determinations at only two pion masses (including the experimental value) a polynomial fit function is chosen,

$$m_\pi r = A + B m_\pi + \cdots. \tag{7}$$

In Fig. 11, the results of our LQCD calculations of $m_\pi r$ are shown, along with the experimental value in each channel and a fit to the form given in Eq. (7). While the uncertainties in the lattice determinations are somewhat large compared to those of the experimental determination, it appears that there is modest dependence upon the light-quark masses. The fit values are

$$\begin{aligned} A^{(^1S_0)} &= 1.348^{+0.080+0.079}_{-0.080-0.083}\,, & B^{(^1S_0)} &= 4.23^{+0.55+0.59}_{-0.56-0.57}\ \text{GeV}^{-1}, \\ A^{(^3S_1)} &= 0.726^{+0.065+0.072}_{-0.059-0.059}\,, & B^{(^3S_1)} &= 3.70^{+0.42+0.42}_{-0.47-0.52}\ \text{GeV}^{-1}. \end{aligned} \tag{8}$$

The two-parameter fit is clearly oversimplistic, and more precise LQCD calculations are required at smaller light-quark masses to better constrain the light-quark mass dependence of the effective ranges.

VI. FINE TUNINGS AND SU(4) SPIN-FLAVOR SYMMETRY

At the physical values of the quark masses, the deuteron is an interesting system as it is much larger than the range of the nuclear force. Its binding energy is determined by the pole in the scattering amplitude in the $^3S_1$-$^3D_1$ coupled channels. It is known very precisely at the physical light-quark masses, $B_d = 2.224644(34)$ MeV, and recently LQCD calculations

TABLE III. Results from the lowest-lying continuum states in the $^3S_1$ channel.

Ensemble	$\lvert\mathrm{P}\rvert$	$b\Delta E$	$\lvert\mathbf{k}\rvert/m_\pi$	$k\cot\delta/m_\pi$	δ (°)
$24^3 \times 48$	0	0.0306(16)(23)	0.324(8)(12)	$0.065^{+0.031+0.47}_{-0.029-0.40}$	78.6(4.7)(6.9)
$24^3 \times 48$	1	0.142(23)(20)	0.6708(60)(54)	$-3.03^{+1.1+0.73}_{-4.0-9.3}$	$-12.5^{+7.1+6.5}_{-6.9-6.1}$
$32^3 \times 48$	0	0.0115(17)(23)	0.198(15)(19)	−0.069(32)(43)	109(9)(13)
$32^3 \times 48$	1	0.0788(24)(40)	0.496(9)(14)		−1(13)(22)
$48^3 \times 64$	0	−0.0011(17)(24)			
$48^3 \times 64$	1	0.0153(30)(49)	0.200(27)(44)		

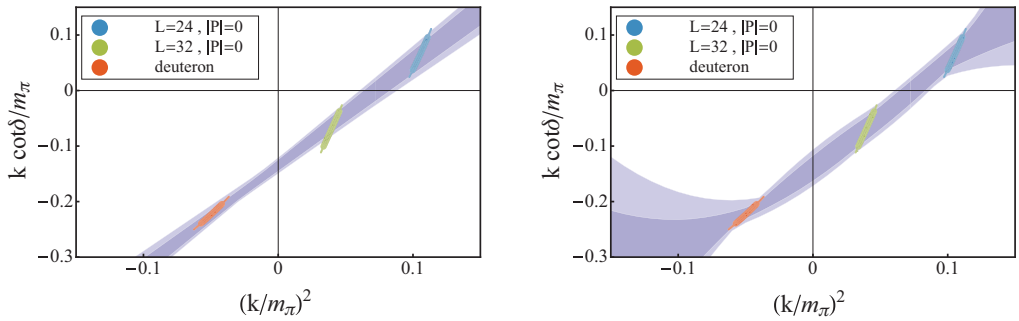

FIG. 8. (Color online) $k \cot \delta$ in the $^3S_1$ channel. The left panel is a two-parameter fit to the ERE, and the right panel is a three-parameter fit to the ERE, as described in the text. The positive energy values are given in Table III and the negative energy value is determined from the deuteron binding energy. The inner (outer) shaded region corresponds to the statistical uncertainty (statistical and systematic uncertainties combined in quadrature).

of the deuteron binding have been performed at unphysical light-quark masses [8,11,13,14]. Given that both the scattering lengths and effective ranges calculated in this work are large compared with the pion Compton wavelength (which naively dictates the range of the interaction for light pions), we explore the naturalness of the two-nucleon systems. In this context, naturalness is defined by the length scales of the system as compared to the range of the interaction. By contrast, a fine-tuned quantity is one in which the length scales of the system are unnatural over a small range of parameters of the underlying theory.

The left panel of Fig. 12 gives the ratio of the scattering length to effective range in the $^3S_1$ channel as a function of the pion mass. As the effective range is a measure of the range of the interaction, this figure reveals that the deuteron is becoming more natural at heavier light-quark masses. In the right panel of Fig. 12, the deuteron binding momentum γ_d (related to the binding energy by $B_d = \gamma_d^2/M_N$) normalized to the pion mass is shown as a function of the pion mass. In the chiral regime one would expect that that γ_d scales as m_π^2 as suggested by effective field theory [44–51]. However, at the heavy up and down quark masses used here, naive expectations based on the uncertainty principle suggest that the deuteron binding momentum, if natural, would scale roughly as the inverse of the range of the interaction. As the ratio of γ_d to m_π as a function of m_π is not constant, but rather is falling, we conclude that pion exchange is no longer the only significant contribution to the long-range component of the nuclear force, consistent with the meson spectrum found at these quark masses.

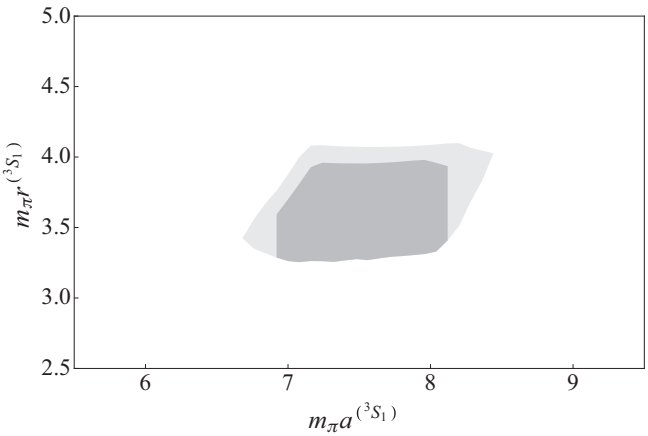

FIG. 9. The 68% confidence region associated with $m_\pi a^{(^3S_1)}$ and $m_\pi r^{(^3S_1)}$ in the $^3S_1$ channel. The inner region corresponds to statistical uncertainties and the outer region corresponds to statistical and systematic uncertainties combined in quadrature.

While more precise calculations at these quark masses are desirable, and LQCD calculations at other light-quark masses and at other lattice spacings are required to make definitive statements, the present calculations suggest that the deuteron remains unnatural over a large range of light-quark masses. This would imply that the unnaturalness of the deuteron binding energy at the physical point is a generic feature of QCD with three light quarks and does not result from a fine-tuning of their masses. If subsequently confirmed, this would be a very interesting result.

The $^1S_0$ channel is unnatural at the physical point with a very large scattering length, but the system appears to be more natural at heavier pion masses. Nonetheless, as shown in Fig. 13 (left panel), the scattering length is approximately twice the effective range at a pion mass of $m_\pi \sim 800$ MeV, similar to the $^3S_1$ channel. In the right panel of Fig. 13, the dineutron binding momentum γ_{nn} (related to the binding energy by $B_{nn} = \gamma_{nn}^2/M_N$) normalized to the pion mass is shown as a function of the pion mass. As in the $^3S_1$ channel, it appears that the pion is not providing the only significant contribution to the long-range component of the nuclear force. However, in contrast to the $^3S_1$ channel, the $^1S_0$ channel is clearly finely tuned at the physical light-quark masses. The range of light-quark masses over which it is fine-tuned requires further LQCD calculations to determine, and eventual consideration of isospin violating effects due to light-quark mass differences and electromagnetism. However, given the experimental determinations of the nn, np and pp scattering lengths, these effects are expected to be small.

It is interesting to note that the ratio of the scattering length to the effective range in the two channels have very similar values at the quark masses used in this work:

$$a^{(^3S_1)}/r^{(^3S_1)} = 2.06^{+0.22+0.25}_{-0.18-0.19}, \quad a^{(^1S_0)}/r^{(^1S_0)} = 2.02^{+0.23+0.29}_{-0.19-0.18}, \tag{9}$$

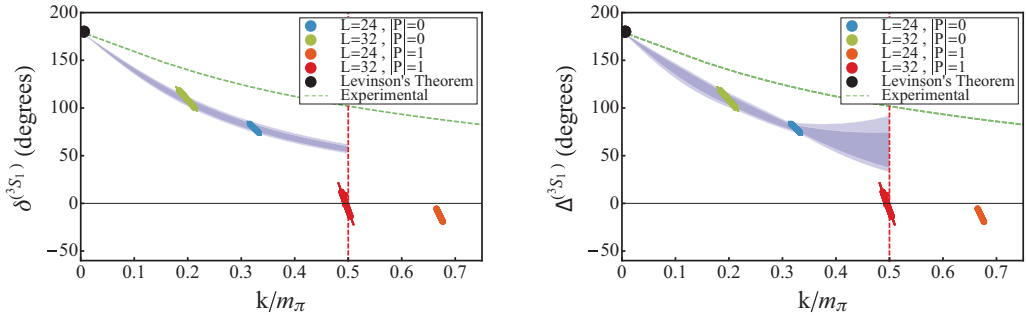

FIG. 10. (Color online) The phase shift in the $^3S_1$ channel. The left panel is a two-parameter fit to the ERE, while the right panel is a three-parameter fit to the ERE, as described in the text. The inner (outer) shaded region corresponds to the statistical uncertainty (statistical and systematic uncertainties combined in quadrature) in two- and three-parameter EREs fit to the results of the lattice QCD calculation. The vertical (red) dashed line corresponds to the start of the t-channel cut and the upper limit of the range of validity of the ERE. The light (green) dashed line corresponds to the phase shift at the physical pion mass from the Nijmegen phase-shift analysis [38].

and that the scattering lengths in the two channels, and also the effective ranges, are within $\sim$20% of each other. In the large-N_c limit of QCD, the nuclear forces in the two spin channels are equal up to corrections suppressed by $\mathcal{O}(1/N_c^2)$ [52], and the two channels transform in the **6** of the Wigner SU(4) symmetry. In addition, inequalities for the binding energies of light nuclei in the Wigner-symmetry limit have been found in Ref. [53]. The closeness of the values of the scattering parameters at $m_\pi \sim 800$ MeV is consistent with the expectations of the large-N_c limit of QCD.

VII. CONCLUSIONS AND DISCUSSIONS

We have presented the results of Lattice QCD calculations of low-energy NN scattering phase-shifts and scattering parameters at the SU(3) symmetric point with a pion mass of $m_\pi \sim 800$ MeV. For the first time, the effective ranges of the NN interactions have been determined using lattice QCD. The calculated scattering lengths and effective ranges indicate that the pion is not the dominant contribution to the long-range part of the nuclear force at these large light-quark masses, as anticipated from the single-hadron spectrum. In both spin channels, the NN phase shifts change sign at higher momentum, near the start of the t-channel cut, indicating that the nuclear interactions have a repulsive core even for heavier quark masses. This suggests that the form of the nuclear interactions, and the effective potentials that will reproduce the scattering amplitude below the inelastic threshold, are qualitatively similar to the phenomenological potentials that describe the experimental scattering data at the physical pion mass.

Both spin channels are, in a sense, more natural at $m_\pi \sim 800$ MeV, where both satisfy $a/r \sim +2.0$, than at the physical pion mass where $a^{(^1S_0)}/r^{(^1S_0)} \sim -8.7$ and $a^{(^3S_1)}/r^{(^3S_1)} \sim +3.1$. The relatively large size of the deuteron compared with the range of the nuclear forces may persist over a large range of light-quark masses, and therefore might, in fact, not be usefully regarded as a fine-tuning in $n_f = 2 + 1$ QCD, but rather a generic feature. The $^1S_0$ channel, in contrast, is finely tuned at the physical light-quark masses and it remains to be seen over what range of masses this persists.

It is interesting to compare the $^1S_0$ and $^3S_1$ scattering lengths found here at the SU(3) symmetric point to those resulting from the few other lattice QCD calculation of the scattering lengths.[4] At pion masses ranging between 354 and 493 MeV [3], both scattering lengths are positive and approximately 1 fm. These results are somewhat in contrast with the naive expectation that the $^3S_1$ scattering length will rise monotonically to its

[4]While there have been quenched determinations of the NN scattering lengths, e.g., as presented in Refs. [1,2,5–7], the leading contribution to the NN interaction in quenched QCD is unphysical and unrelated to QCD [54].

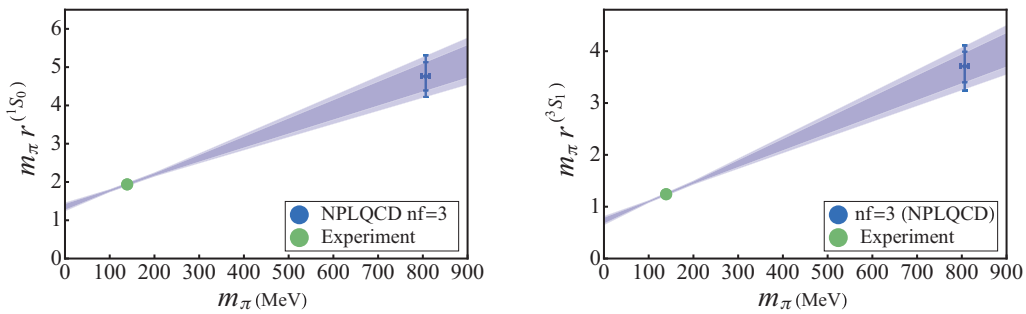

FIG. 11. (Color online) The NN effective range in the $^1S_0$ channel (left panel) and the $^3S_1$ channel (right panel). The inner (outer) shaded region corresponds to the statistical uncertainty (statistical and systematic uncertainties combined in quadrature) in a two-parameter fit to the results of the lattice QCD calculation and the experimental value.

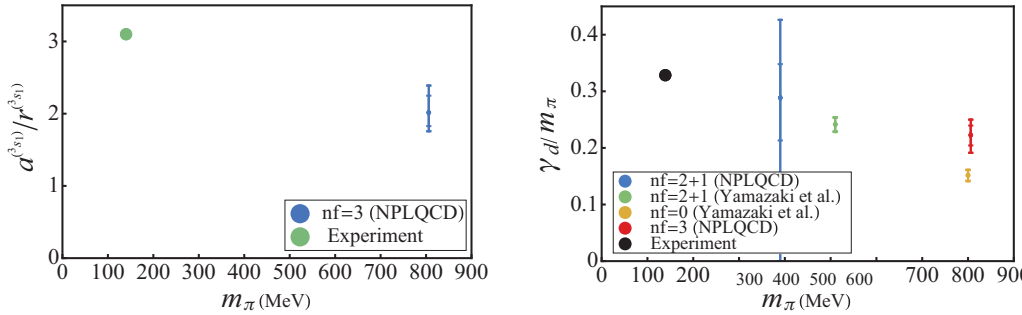

FIG. 12. (Color online) The left panel shows the ratio of the scattering length to effective range in the $^3S_1$ channel. The right panel shows the normalized deuteron binding momentum versus the pion mass [8,11,13,14]. The black point denotes the experimental value.

physical value, and the $^1S_0$ scattering length will approach infinity, as the quark masses approach their physical values. A conclusive resolution of this issue will of course have to await results at lighter quark masses. The HALQCD collaboration finds that both the deuteron and dineutron are unbound at the heavier pion masses [12], in conflict with the results from other groups [11,13,14], and hence the scattering lengths that they find in these channels are incompatible with those found in this work. For instance, at a somewhat heavier pion mass of $m_\pi \sim 700$ MeV, the scattering length in the $^1S_0$ channel has been determined to be $a^{(^1S_0)} = -1.6 \pm 1.1$ fm [55], which is inconsistent at 1σ with our result at the SU(3) symmetric point. For a recent review of the energy splittings calculated in the two-nucleon sector prior to this work, see Ref. [56].

Our calculations were performed at a single pion mass with one lattice spacing and in the absence of electromagnetic interactions. It should be stressed that in the presence of fine-tuning, as in the $^1S_0$ channel at the physical point, lattice-spacing artifacts can be enhanced with respect to expectations based on naive dimensional analysis and scaling arguments. In order to fully explore the behavior of the scattering phase shifts and scattering parameters with fully quantified uncertainties, along with the issues of spin-flavor symmetry and fine tunings, calculations at multiple lattice spacings and smaller light-quark masses are essential and are planned for the future.

ACKNOWLEDGMENTS

We thank R. Edwards and B. Joó for help with QDP++ and CHROMA [57]. We acknowledge computational support from the USQCD SciDAC project, the National Energy Research Scientific Computing Center (NERSC, Office of Science of the US DOE, DE-AC02-05CH11231), the UW HYAK facility, LLNL, the PRACE Research Infrastructure resource CURIE based in France at the Très Grand Centre de Calcul, TGCC, and the NSF through XSEDE resources under Grant No. TG-MCA06N025. S.R.B. and P.J. were partially supported by NSF continuing Grant No. PHY1206498. In addition, S.R.B. gratefully acknowledges the hospitality of HISKP and the Mercator program of the Deutsche Forschungsgemeinschaft. The work of A.P. is supported by Contract No. FIS2011-24154 from MEC (Spain) and FEDER. H.-W.L. and M.J.S. were supported in part by the DOE Grant No. DE-FG03-97ER4014 and by the NSF MRI Grant No. PHY-0922770 (HYAK). K.O. was supported in part by DOE Grants No. DE-AC05-06OR23177 (JSA) and No. DE-FG02-04ER41302. W.D. was supported by the US Department of Energy under cooperative research agreement Contract No. DE-FG02-94ER40818 and by the DOE with the Outstanding Junior Investigator program, No. DE-SC000-1784. The work of T.L. was performed under the auspices of the US Department of Energy by LLNL under Contract No. DE-AC52-07NA27344. The work of A.W.L. was supported in part by the Director, Office of Energy Research, Office of High Energy and Nuclear Physics, Divisions of Nuclear Physics, of the US DOE under Contract No. DE-AC02-05CH11231. M.J.S. thanks the Alexander von Humboldt foundation for the award that enabled his visit to the University of Bonn, and the kind hospitality of Ulf Meißner and the Helmhotz-Institut für Strahlen- und Kernphysik at the University of Bonn.

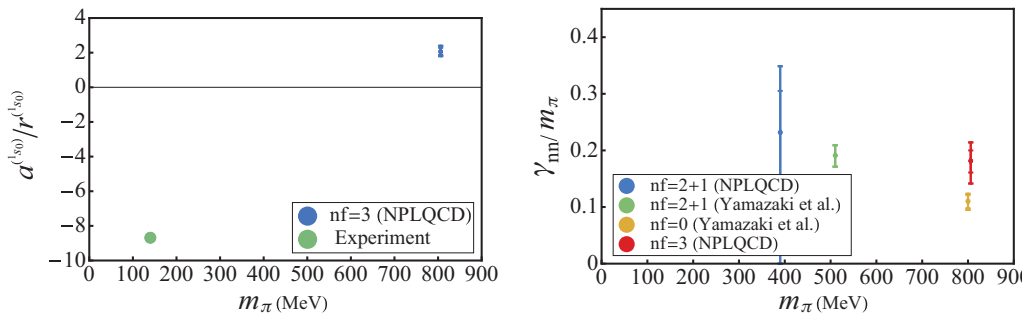

FIG. 13. (Color online) The left panel shows the ratio of the scattering length to effective range in the $^1S_0$ channel. The right panel shows the normalized dineutron binding momentum versus the pion mass [8,11,13,14].

[1] M. Fukugita, Y. Kuramashi, H. Mino, M. Okawa, and A. Ukawa, Phys. Rev. Lett. **73**, 2176 (1994).
[2] M. Fukugita, Y. Kuramashi, M. Okawa, H. Mino, and A. Ukawa, Phys. Rev. D **52**, 3003 (1995).
[3] S. R. Beane, P. F. Bedaque, K. Orginos, and M. J. Savage, Phys. Rev. Lett. **97**, 012001 (2006).
[4] S. R. Beane *et al.* (NPLQCD Collaboration), Phys. Rev. D **81**, 054505 (2010).
[5] N. Ishii, S. Aoki, and T. Hatsuda, Phys. Rev. Lett. **99**, 022001 (2007).
[6] S. Aoki, T. Hatsuda, and N. Ishii, Comput. Sci. Dis. **1**, 015009 (2008).
[7] S. Aoki, T. Hatsuda, and N. Ishii, Prog. Theor. Phys. **123**, 89 (2010).
[8] T. Yamazaki, Y. Kuramashi, and A. Ukawa (PACS-CS Collaboration), Phys. Rev. D **84**, 054506 (2011).
[9] T. Yamazaki, Y. Kuramashi, and A. Ukawa, Phys. Rev. D **81**, 111504 (2010).
[10] P. de Forcrand and M. Fromm, Phys. Rev. Lett. **104**, 112005 (2010).
[11] S. R. Beane *et al.* (NPLQCD Collaboration), Phys. Rev. D **85**, 054511 (2012).
[12] T. Inoue *et al.* (HAL QCD Collaboration), Nucl. Phys. A **881**, 28 (2012).
[13] S. R. Beane, E. Chang, S. D. Cohen, W. Detmold, H. W. Lin, T. C. Luu, K. Orginos, A. Parreno *et al.* (NPLQCD Collaboration), Phys. Rev. D **87**, 034506 (2013).
[14] T. Yamazaki, K.-i. Ishikawa, Y. Kuramashi, and A. Ukawa, Phys. Rev. D **86**, 074514 (2012).
[15] B. Sheikholeslami and R. Wohlert, Nucl. Phys. B **259**, 572 (1985).
[16] S. R. Beane *et al.* (NPLQCD Collaboration), Phys. Rev. D **80**, 074501 (2009).
[17] S. R. Beane *et al.* (NPLQCD Collaboration), Phys. Rev. Lett. **106**, 162001 (2011).
[18] S. R. Beane *et al.* (NPLQCD Collaboration), Mod. Phys. Lett. A **26**, 2587 (2011).
[19] S. R. Beane, E. Chang, S. D. Cohen, W. Detmold, H.-W. Lin, T. C. Luu, K. Orginos, A. Parreno *et al.* (NPLQCD Collaboration), Phys. Rev. Lett. **109**, 172001 (2012).
[20] W. Detmold, R. Edwards, B. Joo, T. Luu, S. Meinel, K. Orginos, D. Richards, and A. Walker-Loud (unpublished).
[21] C. Morningstar and M. J. Peardon, Phys. Rev. D **69**, 054501 (2004).
[22] R. Hoffmann, A. Hasenfratz, and S. Schaefer, PoS LAT **2007**, 104 (2007).
[23] R. G. Edwards, B. Joo, and H.-W. Lin, Phys. Rev. D **78**, 054501 (2008).
[24] S. Meinel (private communication).
[25] S. Basak *et al.* (Lattice Hadron Physics (LHPC) Collaboration), Phys. Rev. D **72**, 074501 (2005).
[26] S. R. Beane, W. Detmold, T. C. Luu, K. Orginos, A. Parreno, M. J. Savage, A. Torok, and A. Walker-Loud, Phys. Rev. D **79**, 114502 (2009).
[27] C. Aubin and K. Orginos, AIP Conf. Proc. **1374**, 621 (2011).
[28] K. Orginos, PoS LAT **2010**, 118 (2010).
[29] S. R. Beane, W. Detmold, K. Orginos, and M. J. Savage, Prog. Part. Nucl. Phys. **66**, 1 (2011).
[30] M. C. Birse, arXiv:1208.4807.
[31] M. Lüscher, Commun. Math. Phys. **105**, 153 (1986).
[32] M. Lüscher, Nucl. Phys. B **354**, 531 (1991).
[33] S. R. Beane, P. F. Bedaque, A. Parreno, and M. J. Savage, Phys. Lett. B **585**, 106 (2004).
[34] K. Rummukainen and S. A. Gottlieb, Nucl. Phys. B **450**, 397 (1995).
[35] C. h. Kim, C. T. Sachrajda, and S. R. Sharpe, Nucl. Phys. B **727**, 218 (2005).
[36] N. H. Christ, C. Kim, and T. Yamazaki, Phys. Rev. D **72**, 114506 (2005).
[37] Z. Davoudi and M. J. Savage, Phys. Rev. D **84**, 114502 (2011).
[38] Nijmegen Phase Shift Analysis, http://nn-online.org/
[39] J.-W. Chen, G. Rupak, and M. J. Savage, Nucl. Phys. A **653**, 386 (1999).
[40] S. Weinberg, Phys. Lett. B **251**, 288 (1990).
[41] S. Weinberg, Nucl. Phys. B **363**, 3 (1991).
[42] D. B. Kaplan, M. J. Savage, and M. B. Wise, Phys. Lett. B **424**, 390 (1998).
[43] D. B. Kaplan, M. J. Savage, and M. B. Wise, Nucl. Phys. B **534**, 329 (1998).
[44] S. R. Beane, P. F. Bedaque, M. J. Savage, and U. van Kolck, Nucl. Phys. A **700**, 377 (2002).
[45] S. R. Beane and M. J. Savage, Nucl. Phys. A **713**, 148 (2003).
[46] E. Epelbaum, U.-G. Meißner, and W. Glöckle, Nucl. Phys. A **714**, 535 (2003).
[47] S. R. Beane and M. J. Savage, Nucl. Phys. A **717**, 91 (2003).
[48] E. Braaten and H.-W. Hammer, Phys. Rev. Lett. **91**, 102002 (2003).
[49] V. V. Flambaum and R. B. Wiringa, Phys. Rev. C **76**, 054002 (2007).
[50] J. W. Chen, T. K. Lee, C. P. Liu, and Y. S. Liu, Phys. Rev. C **86**, 054001 (2012).
[51] M. E. Carrillo-Serrano, I. C. Cloet, K. Tsushima, A. W. Thomas, and I. R. Afnan, Phys. Rev. C **87**, 015801 (2013).
[52] D. B. Kaplan and M. J. Savage, Phys. Lett. B **365**, 244 (1996).
[53] J. W. Chen, D. Lee, and T. Schaefer, Phys. Rev. Lett. **93**, 242302 (2004).
[54] S. R. Beane and M. J. Savage, Phys. Lett. B **535**, 177 (2002).
[55] N. Ishii *et al.* (HAL QCD Collaboration), Phys. Lett. B **712**, 437 (2012).
[56] T. Doi (HAL QCD Collaboration), PoS LAT **2012**, 009 (2012).
[57] R. G. Edwards and B. Joo, Nucl. Phys. Proc. Suppl. **140**, 832 (2005).